◆ Human Brain Mapping 30:660–674 (2009) ◆

Hand Somatosensory Subcortical and Cortical Sources Assessed by Functional Source Separation: An EEG Study

Camillo Porcaro,[1,2]* Gianluca Coppola,[3] Giorgio Di Lorenzo,[4] Filippo Zappasodi,[1,5] Alberto Siracusano,[4] Francesco Pierelli,[3] Paolo Maria Rossini,[6,7] Franca Tecchio,[5,7] and Stefano Seri[8]

[1]*AFaR, Center of Medical Statistics and IT, Fatebenefratelli Hospital, Rome, Italy*
[2]*Institute for Advanced Biomedical Technologies (ITAB), "G. D'Annunzio" University, Chieti, Italy*
[3]*University of Rome "Sapienza" Polo Pontino, I.C.O.T. & IRCCS-Neuromed, Pozzilli (IS), Italy*
[4]*Laboratory of Psychophysiology, Psychiatric Clinic, Department of Neuroscience, University of Rome "Tor Vergata", Rome, Italy*
[5]*ISTC, CNR, Rome, Italy*
[6]*Clinica Neurologica, ''Campus Biomedico'' University, Rome, Italy*
[7]*Casa di Cura SAN RAFFAELE Cassino e IRCCS SAN RAFFAELE PISANA, Italy*
[8]*The Wellcome Trust Laboratory for MEG Studies, School of Life and Health Sciences, Aston University, Birmingham, United Kingdom*

Abstract: We propose a novel electroencephalographic application of a recently developed cerebral source extraction method (Functional Source Separation, FSS), which starts from extracranial signals and adds a functional constraint to the cost function of a basic independent component analysis model without requiring solutions to be independent. Five ad-hoc functional constraints were used to extract the activity reflecting the temporal sequence of sensory information processing along the somatosensory pathway in response to the separate left and right median nerve galvanic stimulation. Constraints required only the maximization of the responsiveness at specific latencies following sensory stimulation, without taking into account that any frequency or spatial information. After source extraction, the reliability of identified FS was assessed based on the position of single dipoles fitted on its retroprojected signals and on a discrepancy measure. The FS positions were consistent with previously reported data (two early subcortical sources localized in the brain stem and thalamus, the three later sources in cortical areas), leaving negligible residual activity at the corresponding latencies. The high-frequency component of the oscillatory activity (HFO) of the extracted component was analyzed. The integrity of the low amplitude HFOs was preserved for each FS. On the basis of our data, we suggest that FSS can be an effective tool to investigate the HFO behavior of the different neuronal pools, recruited at successive times after median nerve galvanic stimulation. As FSs are reconstructed along the entire experimental session, directional and dynamic HFO synchronization phenomena can be studied. *Hum Brain Mapp 30:660–674, 2009.* **© 2008 Wiley-Liss, Inc.**

Contract grant sponsor: Italian Department of University and Research (MIUR); Contract grant number: 2005027850; the European IST/FET Integrated Project NEUROBOTICS.

*Correspondence to: Camillo Porcaro, Center of Medical Statistics and Information Technology, AFaR-Associazione Fatebenefratelli per la Ricerca, Fatebenefratelli Hospital, Isola Tiberina, Rome 00186, Italy. E-mail: camillo.porcaro@afar.it

Received for publication 28 June 2007; Revised 26 November 2007; Accepted 3 December 2007

DOI: 10.1002/hbm.20533

Published online 11 February 2008 in Wiley InterScience (www.interscience.wiley.com).

Key words: blind source separation; functional constraint; electroencephalography; somatosensory evoked potential; high frequency oscillations; 600 Hz

INTRODUCTION

The N20 component of the human short-latency somatosensory response elicited by electrical stimulation of the median nerve at the wrist is a marker of stimulus arrival at the primary sensory cortex. It is mainly generated by excitatory postsynaptic potentials (EPSPs) in Brodmann area-3b (BA 3b) pyramidal cells [Allison et al., 1991]. Since the recognition of a sequence preceding and following the N20, several research groups tried to elucidate its precise complex source structure [Abbruzzese et al., 1978; Buchner et al., 1994, 1995a; Cracco and Cracco, 1976; Maccabee et al., 1983, 1986; Rossini et al., 1987, 1997; Scherg, 1992; Stöhr and Riffel, 1982]. A number of studies identified different loci for somatosensory evoked potential (SSEP) generators: from the subcortical P14 and P16, ascribed to sources possibly located respectively in the brainstem and near the thalamus (or thalamo-cortical radiations), to the cortical sources of N20, P22, and N30-P30 (N/P30) peaks with their respective positions and orientations [Abbruzzese et al., 1978; Buchner et al., 1994, 1995a; Cracco and Cracco, 1976; Maccabee et al., 1983, 1986; Rossini et al., 1997; Scherg, 1992; Stöhr and Riffel, 1982]. Although a postcentral origin for the scalp-derived N/P30 complex has been postulated [Allison et al., 1989], current body of evidence from healthy subjects and patients with movement disorders, as well as from intracranial data obtained during deep brain stimulation procedures, suggests that this component is strongly related to the functionality of a more complex cortico/subcortical loop linking basal ganglia, thalamus, supplementary motor area (SMA), premotor area (PMA), and primary motor cortex [Abbruzzese et al., 1978; Cheron et al., 1994; Hallett, 2000; Insola et al., 1999; Pierantozzi et al., 1999; Rossi et al., 2002; Rossini et al., 1989a,b, 1993, 1996; Ulivelli et al., 1999].

Using narrow band-pass digital filtering, the group of Roger Cracco was the first to extract from the wide-band upper and lower limb SSEPs a burst of high frequency oscillations (HFOs) [Maccabee et al., 1983; Rossini et al., 1981]. In following years, Eisen et al. [1984] hypothesized that HFOs reflect "recurrent intrathalamic neuronal networks activity." More recently, dipole source analysis of SSEPs suggested four loci of sequential activation for HFOs: the first is located near the source of the brainstem P14 component, the second is most active near the thalamic P16 component generator, and the third and the fourth are localized at the cortical level with a tangential and radial orientation, respectively [Curio, 2000; Gobbelé et al., 1998; Ozaki and Hashimoto, 2005; Restuccia et al., 2002].

The scalp-recorded cerebral signals time-locked to the external stimulus are mixed and embedded in unstructured noise and other physiological signals uncorrelated to the phenomenon under investigation. Several approaches have been applied to deconvolve this complex relationship. Functional Source Separation (FSS) is a novel approach to the solution of this problem developed by our group [FSS; Barbati et al., 2006, 2007; Porcaro et al., 2008; Tecchio et al., 2007a,b]. This procedure is based on a standard Independent Component Analysis (ICA) algorithm, and biases the extraction towards the source of interest by adding a functional constraint to the standard cost function. The functional constraint is chosen on the basis of some known physiological reactivity properties of the investigated phenomenon. Starting from extracranial data, a single source corresponding to the global maximum of the cost function is extracted for each constraint. Extracted sources are not required to be independent and their temporal and functional characterization is then possible.

The main aim of this study was to verify the suitability of FSS analysis method to extract the activity of the different neuronal pools recruited at early latencies (within 35 ms after stimulus delivery) along the somatosensory pathway. By exploiting a characterizing functional property, FSS procedure can identify the source activity under a variety of experimental conditions. This property is translated in a constraint added with suitable weight to the kurtosis in the cost function, maximized by a simulated annealing procedure. In the present application, the source responsiveness at a-priori defined latencies was chosen based on physiological knowledge on the sequential activation of both the subcortical and cortical sources along the somatosensory pathway. The criteria used to verify the reliability of extracted FSs were as follows: (1) the consistency of the positions of the identified sources with current knowledge about the subcortical and cortical recruitments induced by the sensory volley at the studied latencies. Each FS position was assessed by solving the inverse problem (through single dipole modeling) using the data obtained in the channel space by retroprojecting each FS; (2) the "signal discrepancy" defined as the residual response to the nerve stimulation present in original channels is not explained by the identified source at the corresponding latency. The FSS extraction method requires the a priori knowledge of the "functional properties" to be used as constraints, minimizing the possibility of isolating unexpected or unknown brain activities. Moreover, the validation steps, with a proper localization procedure, should be performed to check for the correctness of the position of the neuronal source, whose time-course activity

can be studied along different experimental states. One inherent benefit of the method is that the activity of each FS is characterized along its entire temporal evolution. We have capitalized on this property to describe and compare the high-frequency oscillation waves embedded in the signal generated at each of the subcortical and cortical neuronal nodes.

Furthermore, we investigated the spatio-temporal properties of HFOs embedded in the signal by exploiting the activation cascade at subcortical and cortical levels as a characterizing functional property.

MATERIALS AND METHODS

Experimental Setup

Six healthy volunteers (3 women and 3 men; mean ± SD age: 28.2 ± 3.1) were recruited from the medical students and healthcare professionals of the department of Psychiatry of "Tor Vergata" University in Rome. Inclusion criteria were absence of any overt medical condition, and in particular, any personal or familial history of neurological and psychiatric illness. Subjects taking any medication on a regular basis were excluded. All participants were given a complete description of the study and granted informed consent, after approval of the project by the Ethics Committee of the University "Tor Vergata."

All recordings were performed in the Laboratory of Psychophysiology in the Psychiatric Clinic, Department of Neuroscience of University of Rome "Tor Vergata." Subjects were seated on a comfortable chair in an illuminated room and asked to remain with eyes open, orienting their gaze to a fixation point and their attention to the stimulated hand. Stability of arousal levels was monitored using the online electroencephalographic (EEG) signal.

Somatosensory evoked potentials were elicited after electrical stimulation (constant current stimulator, Bionen Sas, Florence, Italy) of the median nerve at the wrist, using square wave pulses (0.2 ms width, cathode proximal) with a stimulus intensity set at 1.5 times the motor threshold, and at repetition rate of 4.4 Hz. For each subject, two series of one thousand sweeps, one for each side chosen in random order, were collected.

The signal was amplified by 32-channel EEG device (Galileo MIZAR-sirius, EBNeuro, Florence, Italy) and acquired with GalNT software. EEG was recorded using a 23-channel montage with Ag/AgCl disk electrodes located at FP1, FPz, FP2, F7, F3, Fz, F4, F8, T3, C3, Cz, C4, T4, T5, P3, Pz, P4, T6, O1, Oz, O2, C3′, and C4′ positions. C3′ and C4′ was positioned 2 cm posterior to C3 and C4, respectively. The montage was referenced to auricular electrodes, which were linked after placing a resistor in series with each lead to compensate for any imbalance in impedance between the two auricular electrodes and a ground electrode placed between Fz and Cz. Electrode impedance was kept less than 5 kΩ. Data was collected with a sampling rate of 4,096 Hz after band-pass filtering between 1 and 1,500 Hz and analyzed off-line.

Data Analysis

Signal was reformatted against Fz for the purpose of comparison with the majority of HFO literature [Coppola et al., 2005; Gobbelé et al., 1999, 2000, 2004; Halboni et al., 2000].

A semiautomatic ICA-based procedure [Barbati et al., 2004] was applied to identify and eliminate artifactual noncerebral activities, i.e. eye movements, cardiac activity, and environmental noise (50 Hz powerline, Fig. 1). In this preprocessing step, no dimensionality reduction was performed in estimating ICs. After the identification of artifactual ICs, the "cleaned" data were obtained by retroprojecting all the ICs except for artifactual ones.

Functional source separation

The FSS procedure [Tecchio et al., 2007b] was applied to the continuous EEG data in the 5–1,000 Hz frequency band. FSS is based on an ICA model [fastICA, Hyvarinen et al., 2001] which assumes that the set **X** of EEG signals are obtained as a linear combination of statistically independent non-Gaussian sources **S**, through an unknown mixing matrix **A**:

$$\mathbf{X} = \mathbf{AS} \tag{1}$$

Sources **S** are estimated, up to arbitrary scaling and permutation, by independent components **Y** as:

$$\mathbf{Y} = \mathbf{WX} \tag{2}$$

where the unmixing matrix **W** is estimated along with the independent component **Y**. In the FSS procedure, the contrast function uses explicitly additional information to bias the algorithm search towards a single solution that satisfies physiological assumptions (functional source). The contrast function has the form:

$$F = J + \lambda R_{\mathrm{FS}} \tag{3}$$

where J is kurtosis (generally used in fastICA [Hyvarinen et al., 2001]), R_{FS} accounts for the prior information, chosen properly source by source and λ is a parameter to weight the two parts of the contrast function, which was chosen equal to 1,000 in all cases, as detailed in Porcaro et al. [2008]. Briefly, λ was chosen to both minimize computational time and maximize R_{FS}. For all sources starting from the case $\lambda \geq 100$ the maximum value of the R_{FS} was reached. Moreover, the computational time minimization was reached for $\lambda = 1{,}000$.

FSS extracts one source at a time, maximizing the corresponding constraint. For each source the algorithm starts from the original EEG data matrix **X** [Eq. (2)]. Using this

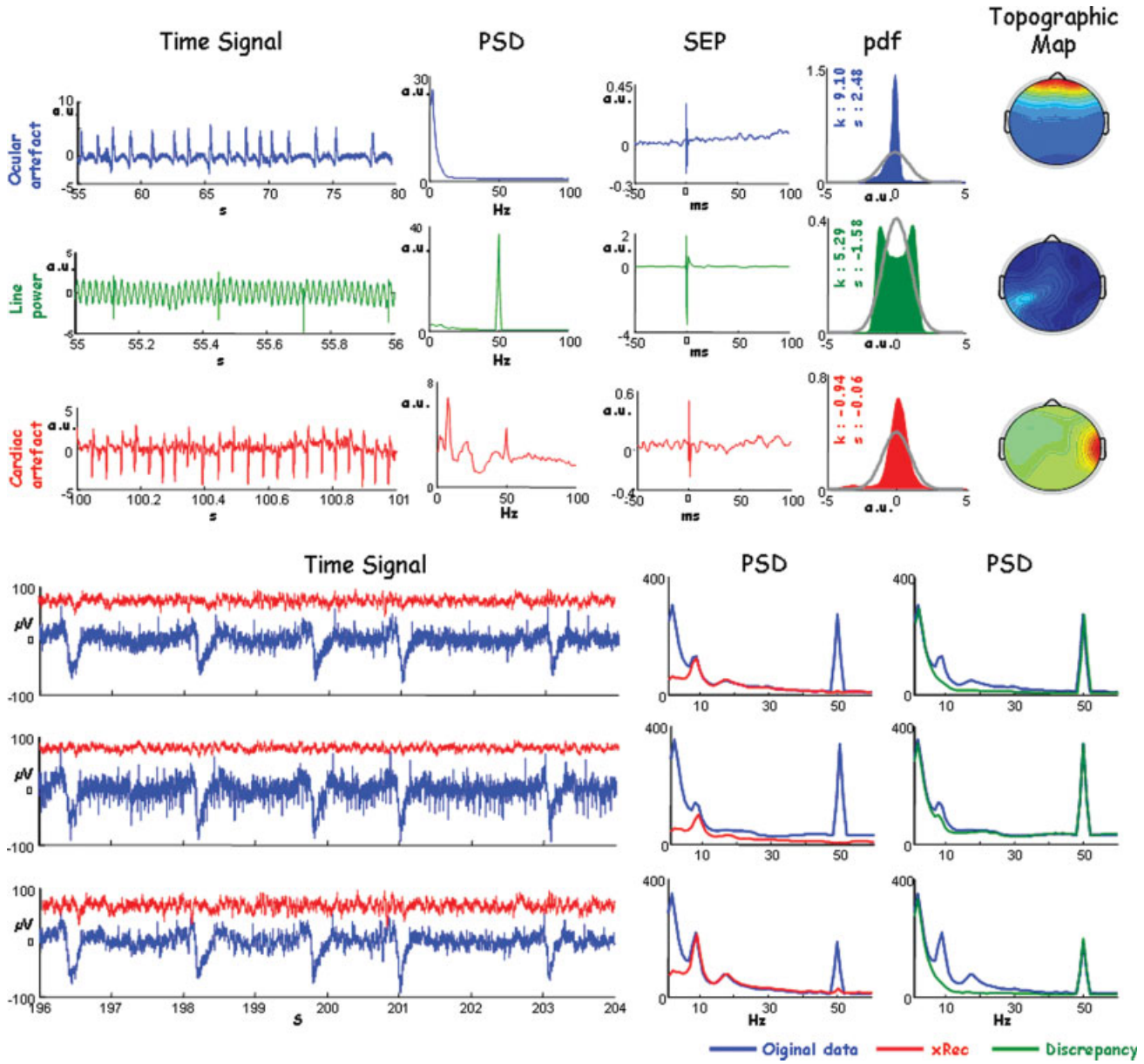

Figure 1.

Artefact identification. Up: First column, time evolution (Time Signal) of the ICs identified as follows: ocular artifact, first row; line power, second row; and cardiac artifact, third row. Time scale is chosen appropriately for each ICs. From second column, for each ICs: the power spectral density (PSD); the average in phase to the median nerve stimulation at wrist (SEP); the probability density function to describe the distribution probability (pdf), the grey line indicates the normal probability density, the values of kurtosis (k), and skewness (s) are provided; spatial distribution obtained by representing the corresponding IC weights (Topographic Map). As ICA procedure performs whitened preprocessing, each quantity is expressed in arbitrary unit (a.u.). Bottom: An exemplificative time segment on three EEG channels, contaminated by different artefacts with different weights. Original signal and PSD (blue), the signals reconstructed by removing all ICs corresponding to different artefacts and its PSD (red); in green the PSD of the signal obtained as retro-projection of only artifactual ICs. [Color figure can be viewed in the online issue, which is available at www.interscience.wiley.com.]

procedure FSS returns each time only the FS with the required property, without an orthogonality constraint. A different functional constraint R_{FS} was defined ad-hoc for each source and the optimization process applied, i.e. the maximization of F by simulated annealing [Barbati et al., 2006].

Five ad-hoc functional constraints R_{FS} were used to extract the activity of the two subcortical and three cortical nodes along the somatosensory network. The functional constraint R_{FS} was defined as:

$$R_{FS_k} = \sum_{t_k-\Delta_1 t_k}^{t_k+\Delta_2 t_k} |EA(t)| - \sum_{6}^{11} |EA(t)| \quad (4)$$

with the evoked activity EA computed by averaging signal epochs of the source FS_k (k = 14, 16, 20, 22, 30), triggered on the median nerve stimulus at wrist (t = 0); t_k is the time point with the maximum electric potential power on the maximal original EEG channel around k ms after the stimulus onset; $\Delta_1\ t_k(\Delta_2\ t_k)$, time point corresponding to a signal amplitude of 50% of the maximal value—by definition in t_k—before (after) t_k; the baseline (no response) was computed in the time interval from 6 to 11 ms. As each source (FS_{14}, FS_{16}, FS_{20}, FS_{22}, and FS_{30}) describes the activity of a neuronal pool recruited at a latencies around 14, 16, 20, 22, and 30 ms, the functional constraint took into account for each maximization the "reactivity" to the stimuli at the corresponding latency. Each latency t_k was chosen for each subject, corresponding to the maximum electric potential power on EEG channel in the time interval of interest.

As only one component is extracted each time from the original data matrix, it is possible to avoid the amplitude indeterminacy inherent the general ICA method. Once the k-th source which optimizes the contrast function F_k had been obtained, the estimated solution was multiplied by the Euclidean norm of its weight vector $\mathbf{a}_{FS_k}$ ($\mathbf{a}_{FS_k}$ such as $\mathbf{a}_{FS_k} = a_{FS_k}\hat{\mathbf{a}}_{FS_k}$, with $|\hat{\mathbf{a}}_{FS_k}| = 1$), allowing amplitude comparisons among sources in a fixed position.

The whole procedure of extraction was performed separately for the trials corresponding to the left and the right nerve stimulation, obtaining five sources for each hemisphere.

FS evaluation

To evaluate the "goodness" of functionally separated sources (FS_{14}, FS_{16}, FS_{20}, FS_{22}, and FS_{30}) in the left and the right hemisphere, two criteria Position and Discrepancy were used.

FS position. To estimate the spatial position of each FS, the source was separately retroprojected, to obtain its field distribution, as follows:

$$\mathbf{EEG}\_\mathrm{rec}_{FS_k} = \mathbf{a}_{FS_k} FS_k \quad (5)$$

where $\mathbf{a}_{FS_k}$ is the estimated mixing vector [matrix $\mathbf{A}$ of Eq. (1)] for the functional source FS_k (FS_k = FS_{14}, FS_{16}, FS_{20}, FS_{22}, FS_{30}) and $\mathbf{EEG}\_\mathrm{rec}_{FS_k}$ are the retroprojection on the sensors channels of the estimated FS_k.

Source localization was performed using an equivalent current dipole (ECD) model, with four concentric conductive spheres (routine DIPFIT2 [Oostenveld and Oostendorp, 2002] of EEGLAB v5.03, available at http://www.sccn.ucsd.edu/eeglab [Delorme and Makeig, 2004]). EEGLAB expresses ECD position in Talairach coordinates and projects them in the template brain of Montreal Neurological Institute (MNI). It is to be noted that the potential distribution obtained by retroprojecting only one component is time-invariant up to a scale factor; consequently, the subtending current distribution shape (ECD position, in our case) is time-independent.

FS discrepancy. To quantify the level of residual response to the nerve stimulation after each source extraction, we defined a "discrepancy response" index as follows:

$$\mathrm{disc}_{FS_k} = \frac{\sum_i \left(\bar{R}^{EEG}_{FS_k} - \bar{R}^{EEG\_rec_{FS}}_{FS_k}\right)^2}{\sum_i \left(\bar{R}^{EEG}_{FS_k}\right)^2} \quad (6)$$

Where $\bar{R}_{FS_k}$ is the reactivity index defined as:

$$\overline{R_{FS_k}} = \frac{R_{FS_k}}{\Delta_2 t_k + \Delta_1 t_k + 1} \quad (7)$$

where R_{FS_k} is defined in Eq. and t_k refers to the latency of each extracted source.

Superscript EEG refers to original data and $\mathrm{EEG\_rec}_{FS_k}$ to the EEG data obtained by retroprojecting each source FS_k (FS_k = FS_{14}, FS_{16}, FS_{20}, FS_{22}, FS_{30}). The index i run upon the four channels of minimal and maximal amplitude at the latency corresponding to the each source.

FS position and discrepancy statistical analysis. General Linear Model (GLM) for repeated measures was used to test for differences in source localization across subjects, with the dependent variable being the 3D dipole coordinate vectors (x, y, z) and the within-subject independent variable was the five-level factor Source (FS_{14}, FS_{16}, FS_{20}, FS_{22}, and FS_{30}). The within subject effect Hemisphere (left, right) was included in the design, to consider possible interhemispheric asymmetries. Therefore, to compare the two hemispheres, since the sagittal plane of Talairach space (the z-y plain) passes through the interhemispheric fissure and the x coordinate is positive or negative depending on the hemisphere, we changed the sign of the x coordinate for the left hemisphere.

For discrepancy, index percentile values were provided.

FS oscillatory activity high-frequency characterization

Even though each source is extracted by exploiting a functional constraint requiring maximal responsiveness at a specific time interval, the corresponding signal is estimated for the entire recording epoch. This enables accurate time-frequency characterization of each FS. For each extracted source, HFOs were obtained by band-pass filtering the signal in the 450–750 Hz frequency range by forward–backward second-order Butterworth filter. The HFO time course for each FS_k was averaged on the stimulus onset.

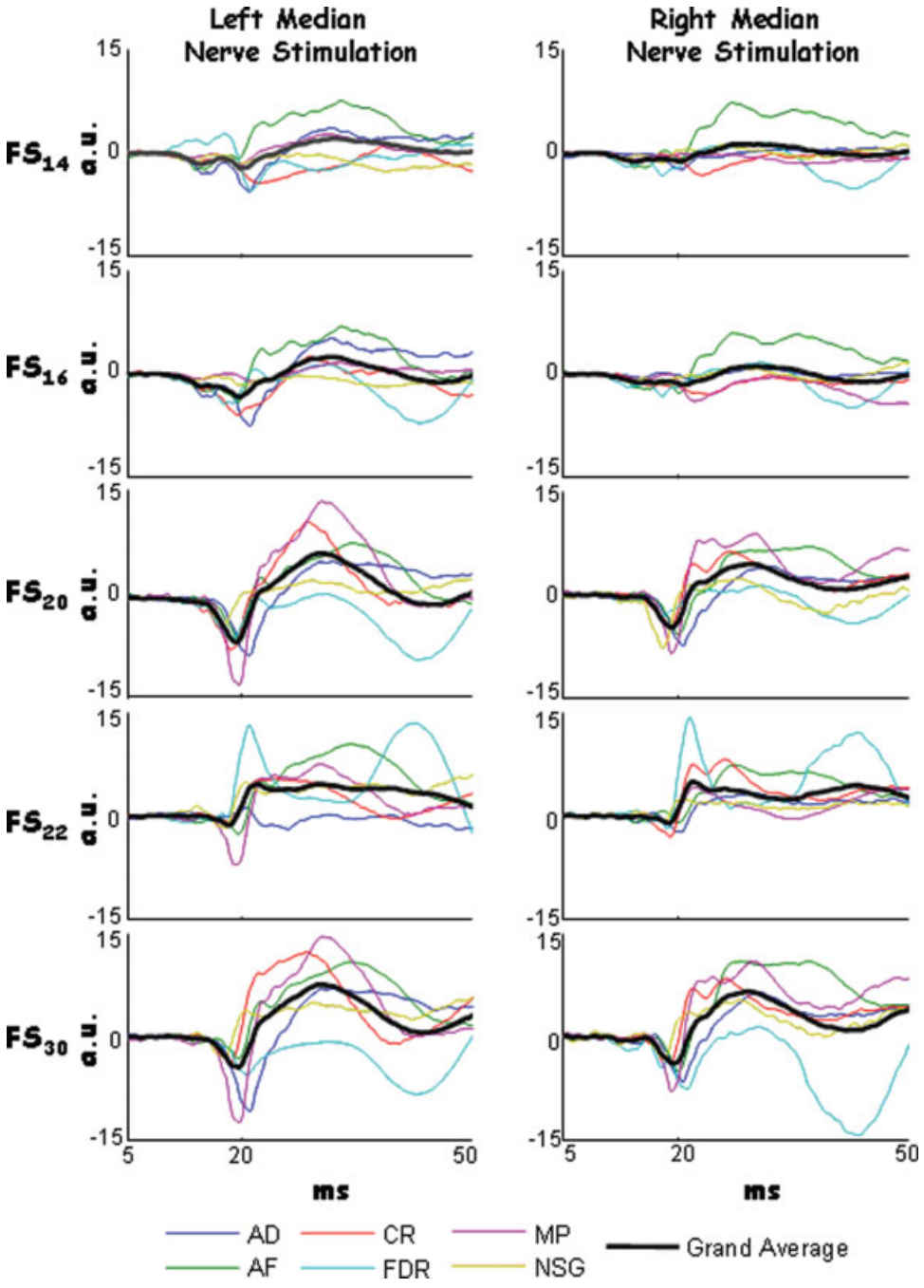

Figure 2.
FS extraction. Time course of the stimulus-averaged FS_{14}, FS_{16}, FS_{20}, FS_{22}, and FS_{30} in the 5–50 ms time period following the galvanic stimulation of left (left column) and right (right column) median nerve for each subject (colour lines). The grand average across subject (black line) is also shown. [Color figure can be viewed in the online issue, which is available at www.interscience.wiley.com.]

RESULTS AND DISCUSSION

Functional Source Separation

In all six subjects, and in both hemispheres, the five functional sources FS_{14}, FS_{16}, FS_{20}, FS_{22}, and FS_{30} were successfully extracted (Fig. 2). Functional source identification depended on accurate latency identification, especially for the subcortical component. We, therefore, manually checked the individual latency of each component for each subject (Table I).

FS Evaluation

Statistical analysis across subject was applied to the 10 FSs, five in the left and five in the right hemisphere.

FS position

All FSs displayed a dipolar potential distribution, similar to that of the original dataset at the corresponding latency

TABLE I. SEP component latencies

	Left arm					Right arm				
	P14	P16	N20	P22	N/P30	P14	P16	N20	P22	N/P30
AD	15,00	16,00	21,00	25,25	32,00	12,75	15,75	20,50	26,50	30,00
AF	14,00	16,00	19,50	26,25	35,00	14,25	16,00	20,00	23,00	32,00
CR	14,00	15,50	19,00	22,00	29,00	13,50	14,75	19,00	22,00	26,00
FDR	12,75	14,75	18,25	21,00	35,00	12,75	14,75	18,25	21,50	32,00
MP	13,50	15,25	19,50	24,50	31,00	13,50	15,25	18,50	22,50	30,50
NSG	12,50	14,00	18,25	22,00	30,00	12,75	14,00	18,25	21,50	26,50
Mean	13,63	15,25	19,13	23,50	32,00	13,25	15,08	19,04	22,83	29,50
Std. dev.	0,92	0,77	1,02	2,12	2,53	0,61	0,74	0,96	1,89	2,65

For each subject, the latency of each component as identified as maximum of the power of the evoked response. In the last rows mean and standard deviation across subjects.

(Fig. 3), confirming the suitability of the single dipole model as inverse solution strategy.

The five sources were located in different positions, as indicated by the significant Source factor [Wilks' Lambda = 0.102, F (12.0, 47.9) = 5.460, $P < 0.0001$, Fig. 4]. Post-hoc comparisons indicated the three coordinates were different for the five sources, that is, x [$F(1,5) = 41.863$, $P < 0.001$], y [$F(1,5) = 6.652$, $P = 0.049$], and the z [$F(1,5) = 22.997$, $P < 0.005$]. The mean position of the ECDs indicated that the FS_{14} and FS_{16} sources were deeper and more medial with respect to the others (FS_{20}, FS_{22}, and FS_{30}), which were localized rostro-laterally (Tables II and III, and Fig. 4). Moreover, FS_{16} was lateral than the FS_{14} (Tables II and III). These results integrated in the MNI space showed a subcortical position of the FS_{14} and FS_{16} and a cortical position of the remaining sources (FS_{20}, FS_{22}, and FS_{30}).

Since the early observations of positive far-field potentials with peak latencies in a range of 13–17 ms [Abbruzzese et al., 1978; Cracco and Cracco, 1976; Maccabee et al., 1983; Stöhr and Riffel, 1982], many authors tried to elucidate their complex origin. The first hypothesis was that they were far-field reflections of the activity of the deep brain regions projecting to the cortex (dorsal columns nuclei, medial lemniscus around 14 ms; the thalamus and the thalamo-cortical radiation around 16 ms). This interpretation was subsequently confirmed by the investigations using high-resolution EEG recordings and dipole source analysis, suggesting independent sources in the brainstem and near the thalamus. In accordance with previous findings, sources corresponding to the N20 and the subsequent P22 and N/P30 components were localized in the peri-rolandic region [Buchner et al., 1995a,1995b; Gobbelé et al., 1998, 2004; Mauguiere et al., 1997; Restuccia et al., 2002; Rossini et al., 1987; Valeriani et al., 1998].

It is worth highlighting that even though no spatial information in the constraint function was used to identify the FSs, and in spite of the limited spatial resolution offered by our 23 channel montage, FSS procedure was able to extract sources with a reasonable spatial accuracy.

FS discrepancy

Median values of the discrepancy indices (Fig. 5) were below 2.4% in response to the left median nerve stimulation and 6.4% to the right (Table II). This confirms that the source extraction was associated with minimal residual activity, i.e. the 10 extracted sources described practically all the evoked response contained in the original EEG data at the corresponding latency.

FSS Procedure

Strengths

The main difference between FSS and other source extraction methods, ranging from inverse problem solving algorithms to spatial filters like beamforming, is that FSS requires no information about the physical relationship between cerebral source generators and their field distribution. Separated FSs provide the source activities in time and the spatial distribution of the electric field they generate, from which appropriate modeling are to be used to solve the inverse problem to know the source position. The solution of the inverse problem theoretically provides in one go both the source position and its time evolution. Unfortunately, at one side it is hill-posed and adjunctive information is to be added, chosen properly time by time. At the other side, the solution is based on the relationship between the current distribution and that of the generated field. This relation depends on physical properties, which are known with low-resolution using information provided by different imaging techniques, requiring complex integration procedures affected by non-zero error. As a consequence, the inverse problem solution is based on the information less accurate provided by the electrophysiological techniques, while FSS algorithms do solve the source identification problem using the most accurate information, i.e. the statistical temporal frequency properties of the signal.

Appropriate models can then be applied to characterize the 3D configuration of the extracted sources. In many

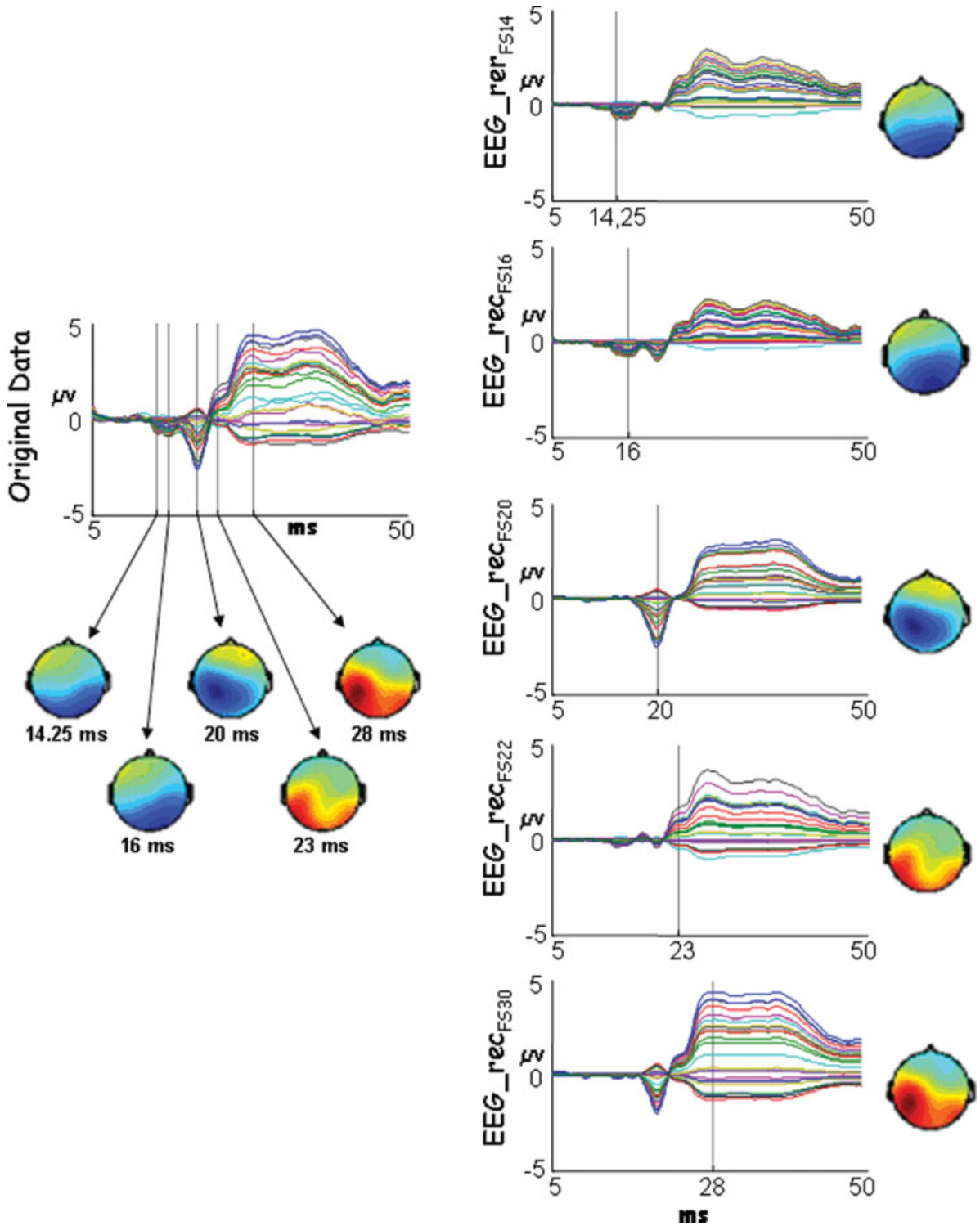

Figure 3.

Topographic map comparison. For a representative subject, Left column: SSEP of right median nerve, obtained as stimulus-locked average of the EEG data, in the 5–50 ms time window following the stimulus onset. The potential distribution on the scalp (topographic map) is shown at the latency corresponding to the first components (P14 at 14.25 ms, P16 at 16 ms, N20 at 20 ms, P22 at 23 ms, N/P30 at 28 ms, vertical lines). Right column: stimulus-locked average of each retro-projected FS (EEG_rec_{FS}, with FS = FS_{14}, FS_{16}, FS_{20}, FS_{22}, and FS_{30}) in the 5–50 ms time window following the stimulus onset. The scalp distribution of the weight matrix is also shown for each extracted source. To be noted that the scalp distribution of the FS weights ($\mathbf{a}_{FS}$, FS = FS_{14}, FS_{16}, FS_{20}, FS_{22} and FS_{30}) is time invariant, i.e. fixed along the whole time evolution, unless a multiplicative factor. [Color figure can be viewed in the online issue, which is available at www.interscience.wiley.com.]

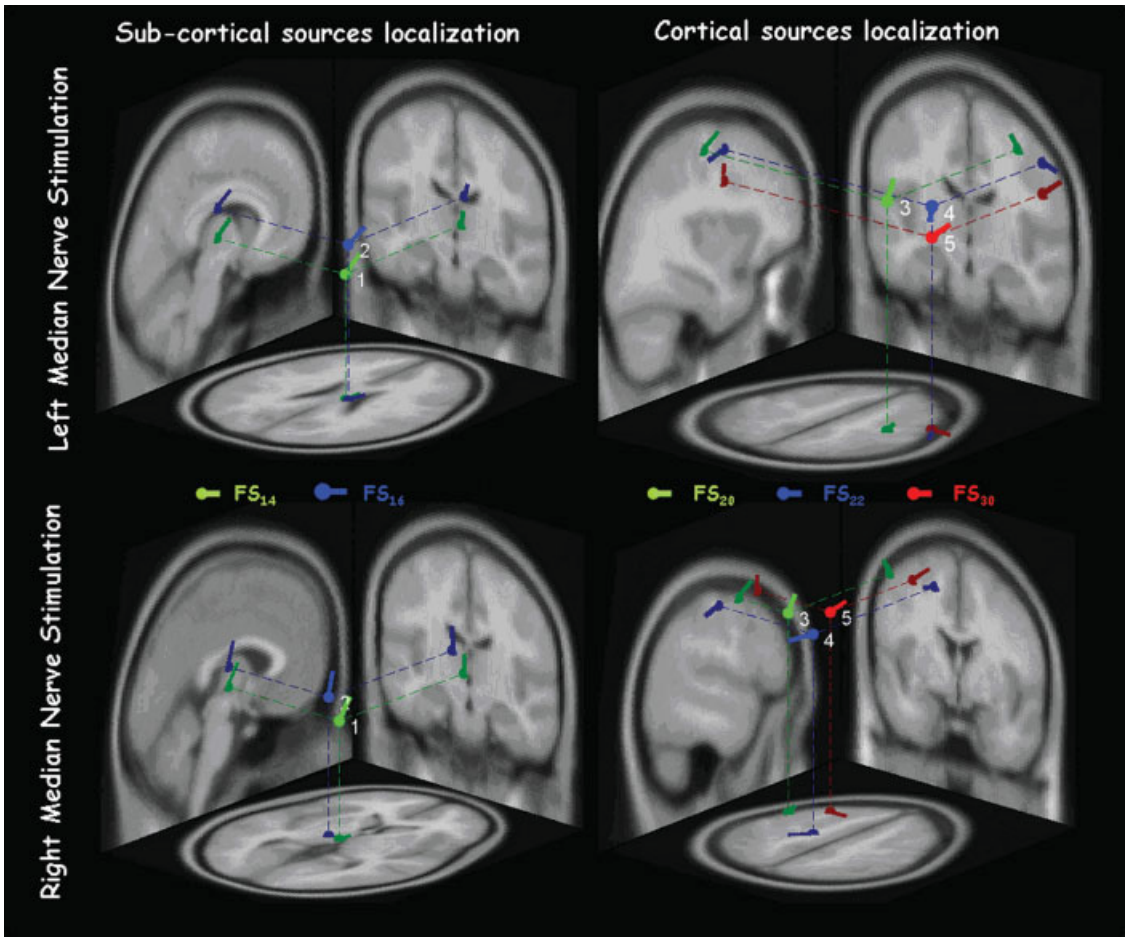

Figure 4.

Single subject FS positions. Position, direction, and orientation of the ECD corresponding to each FS in response to the left and right separate median nerve stimulation, in the MNI brain template—axial, coronal, and sagittal views. [Color figure can be viewed in the online issue, which is available at www.interscience.wiley.com.]

cases, the scientific interest is in the morphological and temporal characteristics of the signal and its modulation in the different experimental conditions. Whenever the source position is of specific interest, FSS allows the use of source localization algorithms having isolated the field distribution generated by the specific source of interest. Moreover, even if a source is extracted by exploiting a functional constraint related to a specific time portion of the experiment,

TABLE II. FSs position and discrepancy

	Right median nerve stimulation					Left median nerve stimulation				
	Position					Position				
	r.v.	x (mm)	y (mm)	z (mm)	Discrepancy (%)	r.v.	x (mm)	y (mm)	z (mm)	Discrepancy (%)
FS_{14}	0.06	−3 [3.62]	−17 [4.48]	2 [4.76]	6.4 [0.8–32.5]	0.08	6 [5.16]	−16 [5.47]	6 [3.11]	2.4 [0.3–14.4]
FS_{16}	0.06	−12 [2.06]	−16 [4.40]	13 [5.13]	3.3 [0.8–16.6]	0.05	8 [6.24]	−15 [5.58]	22 [9.88]	2.0 [0.6–3.8]
FS_{20}	0.14	−34 [4.85]	6 [6.62]	41 [5.70]	0.4 [0.3–5.6]	0.06	31 [4.21]	−5 [4.35]	43 [4.09]	0.2 [0.2–0.6]
FS_{22}	0.03	−34 [8.01]	−15 [0.01]	37 [9.25]	0.7 [0.1–1.6]	0.06	42 [7.36]	−2 [3.68]	35 [3.68]	0.8 [0.5–6]
FS_{30}	0.06	−26 [2.47]	0 [8.03]	32 [5.78]	0.2 [0.1–1.6]	0.04	−31 [2.64]	1 [4.10]	34 [0.11]	0.1 [0.0–0.4]

For each FS in response to the right and left median nerve stimulation, mean position [standard error] (x, y, z) and residual variances (r.v.) across subjects of the corresponding ECD are reported. In the discrepancy columns, the discrepancy median and interquartile ranges, i.e. the values including the central 90% of the distribution [5–95 percentile] are indicated.

TABLE III. Multiple comparisons among FS position coordinates

		FS_{14}	FS_{16}	FS_{20}	FS_{22}	FS_{30}
FS_{14}	*X*	—				
	Y	—				
	Z	—				
FS_{16}	*X*	>0.200	—			
	Y	>0.200	—			
	Z	>0.200	—			
FS_{20}	*X*	<0.0001	0.002	—		
	Y	0.005	0.057	—		
	Z	0.004	0.032	—		
FS_{22}	*X*	0.002	0.002	>0.200	—	
	Y	0.149	0.015	0.174	—	
	Z	0.02	0.003	0.161	—	
FS_{30}	*X*	0.002	>0.0001	>0.200	>0.200	—
	Y	0.098	0.057	>0.200	>0.200	—
	Z	0.006	0.046	0.045	>0.200	—

Paired comparison significance *P* values (see text).

the corresponding estimated signal could be studied all along the length of the whole session.

Limitations

As the method requires a well-known a priori "functional" property, it does not allow the extraction of unexpected or unknown brain activities. Moreover, to maximize the use of the FSS method, we introduce in the experimental paradigm an "ad-hoc" task to make maximally active the property exploited in the cost function (i.e. stimulate the median nerve to identify primary sensory areas, request a period of isometric contraction to identify primary motor areas, or a period of passive visual stimulation to identify primary visual areas). This has the inherent implication of lengthening the experimental session. Moreover, FSS is not effective in the absence of a clear hypothesis about the activation properties, as it is often the case for associative areas involved in complex cognitive functions.

FS Oscillatory Activity High-Frequency Characterization

The morphology of the broad band stimulus-averaged FSs is dominated by the low-frequency signal (Fig. 2). Digital filtering between 450 and 750 Hz reveals a clear HFO amplitude maximum at the characteristic peak latency (Fig. 6). This suggests that the constraint requiring maximal responsiveness at specific latencies, a property shared by both low- and high-frequency source activity components, allows access also to the activity of both high- and low-frequency oscillatory activity along the somatosensory pathway.

It has been suggested that low- and high-frequency oscillatory components are generated by different neuronal pools, because of their functional dissociation [Emerson et al., 1988; Gobbelé et al., 1999, 2000; Halboni et al., 2000; Hashimoto et al., 1999; Klostermann et al., 1998, 1999b; Rossini et al., 1987, 1989a,1989b; Yamada et al., 1988]. Their spatial localization is, however, not easily distinguishable. In particular, by means of MEG, at least one generator of HFOs was localized in area 3b [Curio et al., 1994, 1997; Hashimoto et al., 1996, 1999; Ozaki et al., 1998], in proximity to the generator of the low-frequency N20. Using Principal Component Analysis on EEG signal to improve localization procedure, HFOs were localized at subcortical and even subthalamic sites [Gobbelé et al., 1998, 2004; Restuccia et al., 2002]. The participation of both deep and cortical generators to the genesis of HFOs is supported by the evidence from intracranial recordings [Barba et al., 2004; Klostermann et al., 1999a]. Our data is in line with these observations. We found high-frequency bursts (600 Hz) both from the two subcortical (FS_{14} and FS_{16}) and from the two cortical (FS_{20} and FS_{22}) sources. A further interesting point emerges from our data. The morphology of the two averaged subcortical functional sources (FS_{14} and FS_{16}) extracted from the broad-band signal, despite a congruent localization (Tables II and III and Fig. 4), do not give rise to a clearly identifiable activity (Fig. 2). After the narrow band-pass filtration, we were clearly able to follow the somatosensory information flow from the deepest HFO burst of FS_{14} and FS_{16} up to the cortical FS_{20} and FS_{22} (Fig. 6). In particular, when looking to the HFOs of the two subcortical sources (first two rows in Fig. 6), we can observe that FSS procedure is particularly suitable in identifying relevant subcortical contribution to the sensory processing, being the HFO burst much more evident in the FS than in the original EEG signal. Our procedure does not use the spatial position to identify the source of interest; it rather exploits a suitable functional property (maximal responsiveness at the known time point in the present case). This is expected to make it less vulnerable to the low spatial resolution for deep sources associated with the low spatial sampling of our EEG data. The high sensitivity of FSS to deep HFO sources (first two rows in Fig. 6) seems to confirm this hypothesis.

When we look at the HFOs of the FS_{16} and FS_{20} source activities, we can discriminate two oscillatory bursts—not appreciable in the original EEG signal for the N20 source, see Figure 6—which have been indicated as representative of thalamo-cortical presynaptic and cortical postsynaptic activities [Coppola et al., 2005; Gobbelé et al., 2003]. The HFOs embedded in the rising and descending phases already observed for the N20 [Curio, 2000], have a sufficient temporal separation to allow the differentiation between subcortical and cortical contributions in both the FS_{16} and in the FS_{20} activities (Fig. 6). This complex activation structure, might be interpreted as a result of presynaptic repetitive discharges conducted in the terminal segments of thalamo-cortical axons and postsynaptic contributions from intracortical BA 3b. It has to be noted that the filtering procedure revealed one burst for the FS_{14} (around 14 ms) and one burst for the FS_{22} (around 22 ms) not present in the F_{14}, confirming a mainly subcortical origin for the first and a cortical origin for the latter.

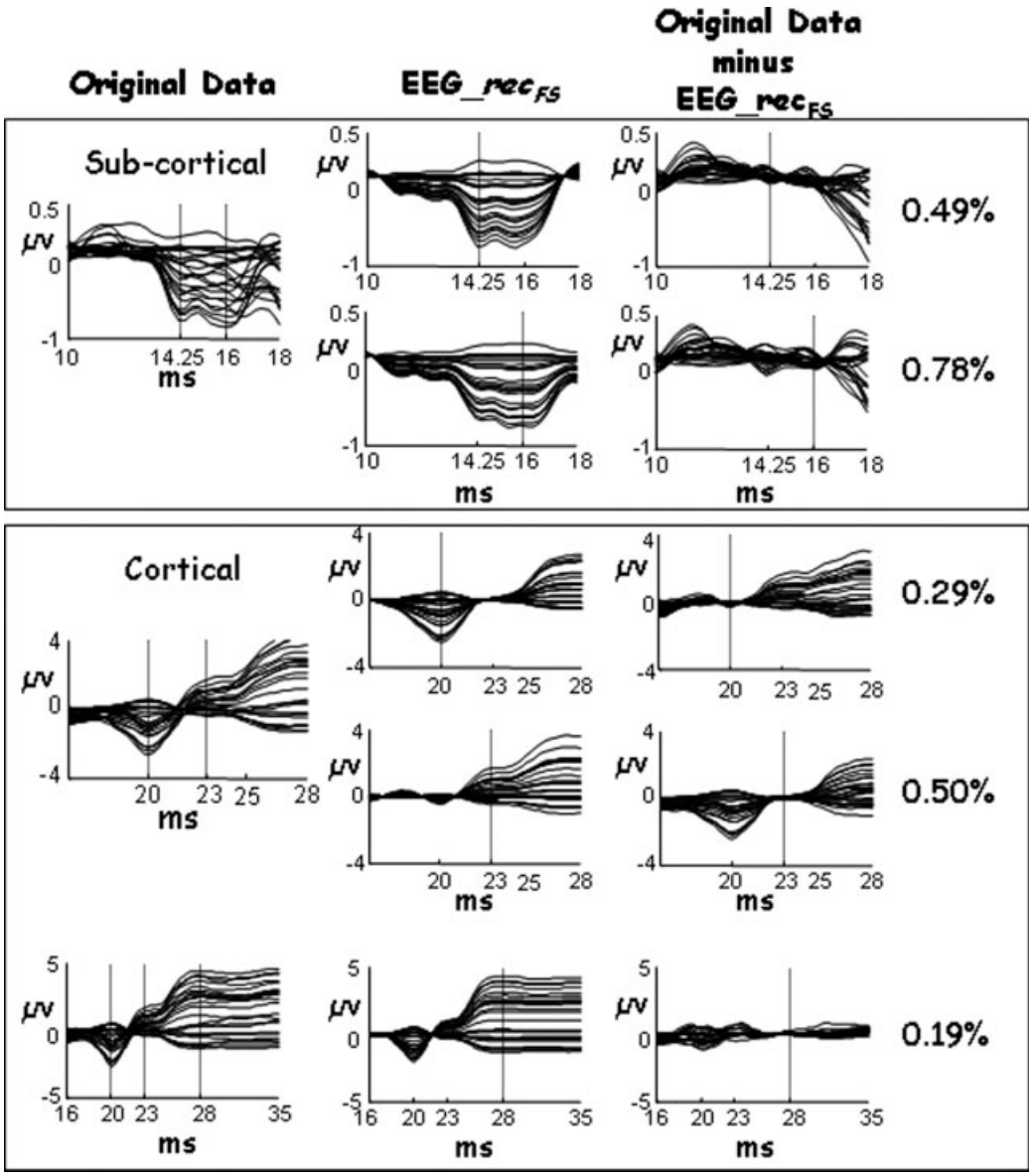

Figure 5.

FS discrepancy. For a representative subject, First column (Original data): SSEP of left median nerve, obtained as stimulus-locked averaging of the EEG data, in a variable time window, optimized to better visualize the morphologic characteristic of the evoked potential components. Boxes differentiated subcortical and cortical components. Second column (EEG_rec$_{FS}$): the average of the retro-projected FS (EEG_rec$_{FS}$, with FS = FS_{14}, FS_{16}, FS_{20}, FS_{22}, and FS_{30}) in the same time windows used in the first column. Vertical line indicated the corresponding latency. Third column (Original data minus EEG_rec$_{FS}$): The original data minus EEG_rec$_{FS}$ (discrepancy) in the same time windows. Values of the discrepancy are also shown. From this example, it is clear how the FSS procedure extracts all the activity in the latency of reactivity where the functional constraint was satisfied.

The high-frequency oscillatory activity of the FS_{30} showed a single burst with a morphology and maximum peak latency quite similar to that of the FS_{22} source. This is in agreement with previous observations that the late somatosensory high frequency oscillations run out in the time interval of the descending slope of N20, sometimes extending into the ascending slope of the N/P30 peak [Coppola et al., 2005].

As a final note, we would like to mention that using FSS procedure, the low-frequency signals and the HFOs could be obtained by simple band pass filtering each source activity. The obtained sources are not required to be inde-

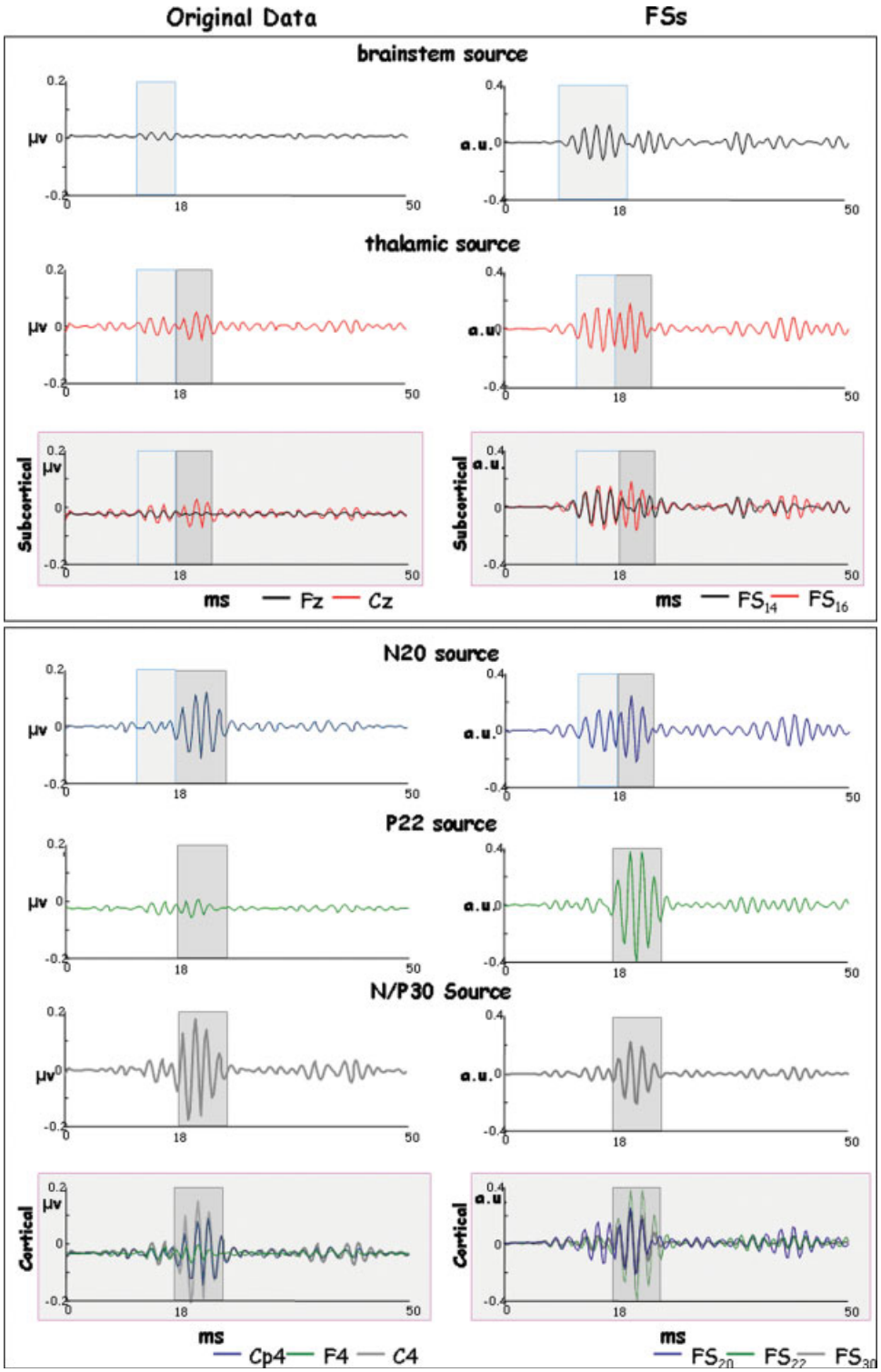

Figure 6.

High-frequency source behavior. For a representative subject, the HFO time course of stimulus-locked average of the five studied sources as characterized by the original EEG data (the maximum channel for each latency peak, left column) and FSs (right column) in the 0–50 ms time window following the stimulus onset. Panels differentiated subcortical (up) and cortical (bottom) components. FS time-series is of higher amplitudes then original data especially for the brainstem and thalamic sources and has a more favorable signal-to-noise ratio. In both the original channels and the FSs, the subcortical components (light blue box) are activated before the cortical ones (grey box) and the thalamic component is still active in correspondence to the N20 source activation. Appreciable in the FS_{20} and not in the original representative channel, a HFO burst preceding the cortical activation. [Color figure can be viewed in the online issue, which is available at www.interscience.wiley.com.]

pendent, as in the standard ICA procedures, and can express physiological activation properties [Barbati et al., 2006]. Moreover, the FS source activities, being reconstructed along the entire experimental session, allow the study of directional and dynamic synchronization phenomena, both at the low- and high- frequency band of oscillatory activity.

CONCLUSION

In this study, the FSS technique has been applied for the first time to EEG signals, in order to extract the activity of the different neuronal pools, recruited at different time intervals after galvanic stimulation of the median nerve. To this aim, five different constraints exploiting dynamical neural recruitment were added to the kurtosis-based cost function of a standard ICA algorithm. Differently from ICA method, FSS does not require independence between extracted sources (the name "component" was changed just to stress that the solutions are no-more independent). Extracted sources localized to the expected cortical and subcortical sites —taking into account the limited spatial sampling of our acquisition—with negligible residual activity and preserved physiological reactivity properties (in the low- and high-frequency ranges of oscillatory activity). FSS approach does require specific functional requirements to identify the source of interest. A wide-range of functional criteria can be used in the extraction procedure. In fact, the use of simulated annealing allows the use of non-differentiable constraints, in addition to the reactivity in different tasks within specific spectrum ranges [Barbati et al., 2007], or maximal reactivity to a specific stimuli at given latencies [Barbati et al., 2006, Porcaro et al., 2008], maximal coherence with a reference signal [Porcaro et al., 2008]. Spatial constraints can be included, although electrophysiological techniques (EEG, MEG) do express their maximal sensitivity in the time and frequency domains, leading to exploit these properties when choosing the functional constraint. Moreover, the FSS procedure, by extracting a single source at a time, does not pose the problem of choosing the "correct" component of interest, as required by ICA methods.

FSS procedure was able to preserve the integrity of the low amplitude, high frequency burst of oscillations in each extracted source activity, thus providing a good tool to investigate the physiological HFO behavior. This has a potential advantage in evaluating effects of an experimental manipulation or clinical condition on the subcortical and cortical nodes along the somatosensory pathway. As FSs are reconstructed along the entire experimental session, directional and dynamic HFO synchronization phenomena can be studied.

ACKNOWLEDGMENTS

The Authors thank Professor GianLuca Romani, Professor Vittorio Pizzella, and Dr. Patrizio Pasqualetti for their continuous support.

REFERENCES

Abbruzzese M, Favale E, Leandri M, Ratto S (1978): New subcortical components of the cerebral somatosensory evoked potential in man. Acta Neurol Scand 58:325–332.

Allison T, McCarthy G, Wood CC, Williamson PD, Spencer DD (1989): Human cortical potentials evoked by stimulation of the median nerve. II. Cytoarchitectonic areas generating long-latency activity. J Neurophysiol 62:711–722.

Allison T, McCarthy G, Wood CC, Jones SJ (1991): Potentials evoked in human and monkey cerebral cortex by stimulation of the median nerve. A review of scalp and intracranial recordings. Brain 114:2465–2503.

Barba C, Valeriani M, Colicchio G, Tonali P, Restuccia D (2004): Parietal generators of low- and high-frequency MN (median nerve) SEPs: Data from intracortical human recordings. Clin Neurophysiol 115:647–657.

Barbati G, Porcaro C, Zappasodi F, Rossini PM, Tecchio F (2004): Optimization of an independent component analysis approach for artifact identification and removal in magnetoencephalographic signals. Clin Neurophysiol 115:1220–1232.

Barbati G, Sigismondi R, Zappasodi F, Porcaro C, Graziadio S, Valente G, Balsi M, Rossini PM, Tecchio F (2006): Functional source separation from magnetoencephalographic signals. Hum Brain Mapp 27:925–934.

Barbati G, Porcaro C, Hadjipapas A, Adjamian P, Pizzella V, Romani GL, Seri S, Tecchio F, Gareth BR: Functional source separation applied to induced visual gamma activity. Hum Brain Mapp (in press).

Buchner H, Adams L, Knepper A, Rüger R, Laborde G, Gilsbach JM, Ludwig L, Reul J, Scherg M (1994): Preoperative localization of the central sulcus by dipole source analysis of early evoked potentials and three-dimensional magnetic resonance imaging. J Neurosurg 80:849–856.

Buchner H, Waberski TD, Fuchs M, Wischmann HA, Beckmann R, Rienäcker A (1995a): Origin of P16 median nerve SEP component identified by dipole source analysis—Subthalamic or within the thalamo-cortical radiation? Exp Brain Res 104:511–518.

Buchner H, Adams L, Muller A, Ludwig I, Knepper A, Thron A, Niemann K, Scherg M (1995b): Somatotopy of human hand somatosensory cortex revealed by dipole source analysis of early somatosensory evoked potentials and 3D-NMR tomography. Electroencephalogr Clin Neurophysiol 96:121–134.

Cheron G, Piette T, Thiriaux A, Jacquy J, Godaux E (1994): Somatosensory evoked potentials at rest and during movement in Parkinson's disease: evidence for a specific apomorphine effect on the frontal N30 wave. Electroencephalogr Clin Neurophysiol 92:491–501.

Coppola G, Vandenheede M, Di Clemente L, Ambrosini A, Fumal A, De Pasqua V, Schoenen J (2005): Somatosensory evoked high-frequency oscillations reflecting thalamo-cortical activity are decreased in migraine patients between attacks. Brain 128:98–103.

Cracco RQ, Cracco JB (1976): Somatosensory evoked potential in man: Far field potentials. Electroencephalogr Clin Neurophysiol 41:460–466.

Curio G (2000): Linking 600-Hz "spikelike" EEG/MEG wavelets ("s-bursts") to cellular substrates. J Clin Neuophysiol 17:377–396.

Curio G, Mackert BM, Burghoff M, Koetitz R, Abraham-Fuchs K, Haerer W (1994): Localization of evoked neuromagnetic 600 Hz activity in the cerebral somatosensory system. Electroencephalogr Clin Neurophysiol 91:483–487.

Curio G, Mackert BM, Burghoff M, Neumann J, Nolte G, Scherg M, Marx P (1997): Somatotopic source arrangement of 600 Hz oscillatory magnetic fields at the human primary somatosensory hand cortex. Neurosci Lett 234:131–134.

Delorme A, Makeig S (2004): EEGLAB: An open source toolbox for analysis of single-trial EEG dynamics including independent component analysis. J Neurosci Methods 134:9–21.

Eisen A, Roberts K, Low M, Hoirch M, Lawrence P (1984): Questions regarding the sequential neural generator theory of the somatosensory evoked potential raised by digital filtering. Electroencephalogr Clin Neurophysiol 59:388–395.

Emerson RG, Sgro JA, Pedley TA, Hauser WA (1988): State-dependent changes in the N20 component oft the median nerve somatosensory evoked potential. Neurology 38:64–67.

Gobbelé R, Buchner H, Curio G (1998): High-frequency (600 Hz) SEP activities originating in the subcortical and cortical human somatosensory system. EEG Clin Neurophysiol 108:182–189.

Gobbelé R, Buchner H, Scherg M, Curio G (1999): Stability of high-frequency (600 Hz) components in human somatosensory evoked potentials under variation of stimulus rate—Evidence for a thalamic origin. Clin Neurophysiol 110:1–5.

Gobbelé R, Waberski TD, Kuelkens S, Sturm W, Curio G, Buchner H (2000): Thalamic and cortical high-frequency (600 Hz) somatosensory-evoked potential (SEP) components are modulated by slight arousal changes in awake subjects. Exp Brain Res 133:506–513.

Gobbelé R, Waberski TD, Thyerlei D, Thissen M, Darvas F, Klostermann F, Curio G, Buchner H (2003): Functional dissociation of a subcortical and cortical component of high-frequency oscillations in human somatosensory evoked potentials by motor interference. Neurosci Lett 350:97–100.

Gobbelé R, Waberski TD, Simon H, Peters E, Klostermann F, Curio G, Buchner H (2004): Different origins of low- and high-frequency components (600 Hz) of human somatosensory evoked potentials. Clin Neurophysiol 115:927–937.

Halboni P, Kaminski R, Gobbelé R, Züchner S, Waberski TD, Töpper R, Buchner H (2000): Sleep-stage dependent changes of high-frequency part of the somatosensory evoked potentials at the thalamus and cortex. Clin Neurophysiol 111:2277–2284.

Hallett M (2000): Disorder of movement preparation in dystonia. Brain 123:1765–1767.

Hashimoto I, Mashiko T, Imada T (1996): Somatic evoked high-frequency magnetic oscillations reflect activity of inhibitory interneurons in the human somatosensory cortex. Electroencephalogr Clin Neurophysiol 100:189–203.

Hashimoto I, Kimura T, Fukushima T, Iguchi Y, Saito Y, Terasaki O, Sakuma K (1999): Reciprocal modulation of somatosensory evoked N20m primary response and high-frequency oscillations by interference stimulation. Clin Neurophysiol 110:1445–1451.

Hyvärinen A, Karhunen J, Oja E (2001): Independent Component Analysis. New York: Wiley.

Insola A, Rossi S, Mazzone P, Pasqualetti P (1999): Parallel processing of sensory inputs: Evidence from parkinsonians patients implanted with thalamic stimulators. Clin Neurophysiol 110:146–151.

Klostermann F, Nolte G, Losch F, Curio G (1998): Differential recruitment of high frequency wavelets (600 Hz) and primary cortical response (N20) in human median nerve somatosensory potentials. Neurosci Lett 256:101–104.

Klostermann F, Funk T, Vesper J, Curio G (1999a): Spatiotemporal characteristics of human intrathalamic high-frequency (>400 Hz) SEP components. NeuroReport 10:3627–3631.

Klostermann F, Nolte G, Curio G (1999b): Multiple generators of 600 Hz wavelets in human SEP unmasked by varying stimulus rates. NeuroReport 10:1625–1629.

Maccabee PJ, Pinkhasov EI, Cracco RQ (1983): Short latency somatosensory evoked potentials to median nerve stimulation: Effect of low frequency filter. Electroencephalogr Clin Neurophysiol 55:34–44.

Maccabee PJ, Hassan NF, Cracco RQ, Schiff JA (1986): Short latency somatosensory and spinal evoked potentials: Power spectra and comparison between high pass analog and digital filter. Electroencephalogr Clin Neurophysiol 65:177–187.

Mauguiere F, Merlet I, Forss N, Vanni S, Jousmaki V, Adeleine P, Hari R (1997): Activation of a distributed somatosensory cortical network in the human brain: A dipole modelling study of magnetic fields evoked by median nerve stimulation. II. Effects of stimulus rate, attention and stimulus detection. Electroencephalogr Clin Neurophysiol 104:290–295.

Oostenveld R, Oostendorp TF (2002): Validating the boundary element method for forward and inverse EEG computations in the presence of a hole in the skull. Hum Brain Mapp 17:179–192.

Ozaki I, Hashimoto I (2005): Neural mechanisms of the ultrafast activities. Clin EEG Neurosci 36:271–277.

Ozaki I, Suzuki C, Yaegashi Y, Baba M, Matsunaga M, Hashimoto I (1998): High frequency oscillations in early cortical somatosensory evoked potentials. Electroencephalogr Clin Neurophysiol 108:536–542.

Pierantozzi M, Mazzone P, Bassi A, Rossini PM, Peppe A, Altibrandi MG, Stefani A, Bernardi G, Stanzione P (1999): The effect of deep brain stimulation on the frontal N30 component of somatosensory evoked potentials in advanced Parkinson's disease patients. Clin Neurophysiol 110:1700–1707.

Porcaro C, Barbati G, Zappasodi F, Rossini PM, Tecchio F (2008): Hand sensory-motor cortical network assessed by functional source separation. Hum Brain Mapp 29:70–81.

Restuccia D, Valeriani M, Grassi E, Mazza S, Tonali P (2002): Dissociated changes of somatosensory evoked low-frequency scalp responses and 600 Hz bursts after single-dose administration of lorazepam. Brain Res 946:1–11.

Rossi S, Tecchio F, Pasqualetti P, Ulivelli M, Pizzella V, Romani G-L, Passero S, Battistini N, Rossini PM (2002): Somatosensory processing during movement observation in humans. Clin Neurophysiol 113:16–24.

Rossini PM, Cracco RQ, Cracco JB and House WJ (1981): Short latency somatosensory evoked potentials to peroneal nerve stimulation: Scalp topography and the effect of different frequency filters. Electroencephalogr Clin Neurophysiol 52:540–552.

Rossini PM, Gigli GL, Marciani MG, Zarola F, Caramia M (1987): Non-invasive evaluation of input-output characteristics of sensorimotor cerebral areas in healthy humans. Electroencephalogr Clin Neurophysiol 68:88–100.

Rossini PM, Narici L, Romani GL, Traversa R, Cecchi L, Cilli M, Urbano A (1989a): Short latency somatosensory evoked responses to median nerve stimulation in healthy humans: Electric and magnetic recordings. Int J Neurosci 46:67–76.

Rossini PM, Babiloni F, Bernardi G, Cecchi L, Johnson PB, Malentacca A, Stanzione P, Urbano A (1989b): Abnormalities of short-latency somatosensory evoked potentials in parkinsonian patients. Electroencephalogr Clin Neurophysiol 74:277–289.

Rossini PM, Caramia D, Bassetti MA, Pasqualetti P, Tecchio F, Bernardi G (1996): Somatosensory evoked potentials during the ideation and execution of individual finger movements. Muscle Nerve 19:191–202.

Rossini PM, Babiloni F, Babiloni C, Ambrosini A, Onorati P, Urbano A (1997): Topography of spatially enhanced human short-latency somatosensory evoked potentials. NeuroReport 8:991–994.

Scherg M (1992): Functional imaging and localization of electromagnetic brain activity. Brain Topogr 5:103–111.

Stöhr M, Riffel B (1982): Short-latency somatosensory evoked potentials to median nerve stimulation: Components N13-P13, N14-P14, P15, P16 and P18 with different recording methods. J Neurol 228:39–47.

Tecchio F, Graziadio S, Barbati G, Sigismondi R, Zappasodi F, Porcaro C, Valente G, Balsi M, Rossini PM (2007a): Somatosensory dynamic gamma-band synchrony: A neural code of sensorimotor dexterity. Neuroimage 35:185–193.

Tecchio F, Porcaro C, Barbati G, Zappasodi F (2007b): Functional source separation and hand cortical representation for brain-computer interface feature extraction. J Physiol 580:703–721.

Valeriani M, Restuccia D, Di Lazzaro V, Le Pera D, Barba C, Tonali P, Mauguiere F (1998): Dipolar sources of the early scalp somatosensory evoked potentials to upper limb stimulation. Effect of increasing stimulus rates. Exp Brain Res 120:306–315.

Ulivelli M, Rossi S, Pasqualetti P, Rossini PM, Ghiglieri O, Passero S, Battistini N (1999): Time course of frontal somatosensory evoked potentials. Relation to L-dopa plasma levels and motor performance in PD. Neurology 53:1451–1457.

Yamada T, Kameyama S, Fuchigami Y, Nakazumi Y, Dickins QS, Kimura J (1988): Changes of short latency somatosensory evoked potential in Electroencephalogr Clin Neurophysiol 70:126–136.